Published in final edited form as:
Circ Res. 2009 February 13; 104(3): 398–402. doi:10.1161/CIRCRESAHA.108.187724.

Fate Of Culture-Expanded Mesenchymal Stem Cells in The Microvasculature:

In Vivo Observations of Cell Kinetics

Catalin Toma, **William R. Wagner**, **Shivani Bowry**, **Abigail Schwartz**, and **Flordeliza Villanueva**
Cardiovascular Institute (C.T., S.B., A.S., F.V.) and the McGowan Institute of Regenerative Medicine (W.R.W.), University of Pittsburgh School of Medicine, Pa.

Abstract

Vascular delivery of mesenchymal stem cells (MSCs) following myocardial infarction is under clinical investigation. Little is known about the microvascular fate of MSCs. We used intravital microscopy of rat cremaster muscle microcirculation to track intraarterially delivered MSCs. Rat MSCs (average diameter, 23 μm) were bolused into the ipsilateral common iliac artery. Interrogation of an arteriole–venule pair revealed that 92 ± 7% (n = 6) of MSCs arrest and interrupt flow during first pass at the precapillary level, resulting in decreased flow in the feeding arteriole (velocity decreased from 6.3 ± 1.0 to 4.6 ± 1.3 mm/sec; $P<0.001$). MSC deformability evaluated using filtration through polycarbonate membranes revealed that the cortical tension of MSCs (0.49 ± 0.07 dyne/cm, n = 9) was not different from that of circulating mononuclear cells (0.50 ± 0.05 dyne/cm, n = 7). When intravital microscopy was performed 3 days following injection, the number of MSCs in the cremaster further decreased to 14% of the initial number, because of cell death in situ. In vivo labeling of the basement membrane revealed that at 1 day, the surviving cells were spread out on the luminal side of the microvessel, whereas at 3 days, they integrated in the microvascular wall. Despite their deformability, intraarterially delivered MSCs entrap at the precapillary level because of their large size, with a small proportion of surviving MSCs integrating in a perivascular niche.

Keywords

mesenchymal stem cells; microcirculation; ischemia

Bone marrow–derived mesenchymal stem cells (MSCs) are prominent candidates for cell-based cardiac repair based on their immune allotolerance, paracrine effects,[1,2] and expandability in culture.[3] MSC-like cells have been isolated from the circulation, suggesting they can circulate freely, although this concept remains controversial in humans.[4] These findings, coupled with the proposed capacity of MSCs to home to sites of injury,[1] have led to clinical exploration of intravascular delivery of these cells for the treatment of graft-versus-host disease[5] and myocardial infarction.[6,7]

Correspondence to Catalin Toma, MD, University of Pittsburgh Medical Center, 200 Lothrop St, A-332, Pittsburgh, PA 15213. tomac@upmc.edu.

Disclosures
None.

Remarkably, little is known about the biodistribution of MSCs when delivered systemically. A potential problem in this regard is their large size, which can lead to ischemia.[8,9] When administered intravenously, most of the MSCs are trapped in the lungs,[9–11] reducing delivery to, and engraftment at, target sites.[9,11] It is unclear whether MSC arrest in a vascular territory is a mechanical phenomenon or dependent on active adhesion to the endothelium. In vitro MSCs exhibit rolling behavior and endothelial adhesion via P-selectin[12] and very late antigen-4/vascular cell adhesion molecule-1 interactions,[12,13] respectively. It has been proposed that transendothelial migration can occur in a manner similar to that of leukocytes[13] with participation of secreted matrix metalloproteinases[14]; however, direct intravital observations of extravascular migration are lacking.

Optimization of therapeutic strategies for the vascular delivery of MSCs will require an understanding of what physically happens to these cells after systemic injection. We used intravital microscopy to observe the fate of MSCs in the normal microcirculation following arterial delivery, both acutely and chronically. This approach allowed real-time evaluation of cellular interactions under conditions that preserve local microvessel architecture.

Materials and Methods

Cell Lines

Passage 6 Lewis rat MSCs (Tulane University, New Orleans, La) were expanded in culture using α-MEM medium supplemented with 4 mmol/L L-glutamine, antibiotics, and 20% FBS (Atlanta Biologicals). The cells were used up to passage 10 and <80% confluence and maintained in culture up to 10 days per passage. The MSCs were fluorescently labeled with 1 μmol/L 5′chloromethylfluorescein diacetate (CMFDA) (Invitrogen) and resuspended in PBS (10^6 cells/mL). Rat venous blood mononuclear cells (MNCs) were obtained using standard Ficoll gradient separation.

Intravital Microscopy Preparation

Animal experiments were approved by the University of Pittsburgh Institutional Animal Care and Use Committee. Adult Wistar rats (150 to 250 g) were sedated with intraperitoneal pentobarbital sodium (50 mg/kg). The cremaster muscle was exteriorized for intravital microscopy.[15] For cell injection, a 34-gauge cannula was inserted into the common femoral artery ipsilateral to the exteriorized cremaster muscle and advanced to the common iliac artery. Fluorescently labeled MSCs were injected, and the cremaster preparations were examined using fluorescence and DIC microscopy acutely or after 6 to 48 hours (see the expanded Materials and Methods section, available in the online data supplement at http://circres.ahajournals.org).

Measurement of Cell Deformability

The bolus filtration method[16] was used to derive a size-independent index of rat MSC and circulating MNC deformability based on the pressure required to push the cells though membrane pores slightly smaller than the cell size (see the expanded Materials and Methods section).

Statistical Analysis

Data are reported as means ± SEM. For paired comparisons, 2-tailed *t* testing was performed. One-way ANOVA was used ascertain a significant difference ($P<0.05$) among groups, with post hoc Tukey test to determine wherein the differences resided.

Results

Acute Fate of Arterially Injected MSCs

In the 6 rats studied, 92 ± 7% of the injected MSCs (fractional plugging) became arrested in the cremaster muscle during the first pass, resulting in cessation of flow in the plugged microvessels (Figure 1a and 1c and supplemental Video 1) and a decrease in RBC velocity in the feeding resistance artery (from 6.3 ± 1.0 to 4.6 ± 1.3 mm/sec, $P<0.001$), indicating a 27% reduction of flow relative to baseline (Figure 1b). The fluorescent MSCs entrapped exclusively at the precapillary level. By 5 minutes after intraarterial injection, freely circulating MSCs were no longer present. No extravascular migration of MSCs was seen during time lapse measurements made up to 2 hours after injection (Figure 1d). Sodium nitroprusside (SNP) caused vasodilatation in third- and fourth-order arteriolar branches (11.9 ± 3.5% increase in diameter, n = 4), but this did not affect the extent of MSC entrapment (fractional plugging with SNP 91 ± 4%, P = NS versus baseline).

Physical Properties of MSCs

The suspended MSCs (diameter, 23.6 ± 0.7 μm; average of 4 different passage 9 cell preparations with at least 50 random measurements per preparation) were larger than the cremaster muscle capillaries (7.2 ± 0.3 μm) and circulating MNCs (7.7 ± 0.4 μm), whereas arrested MSCs in the cremaster (11.5 ± 1.2 μm in the minor axis) were larger than the capillaries.

Figure 2 shows the data for the deformability studies. For rat circulating MNCs a p_{yield} of 1.08 ± 0.2 mm Hg corresponded to a cortical tension of 0.50 ± 0.05 dyne/cm (n = 7, Figure 2a). Even with using larger pores (10 μm), only 39.4% of the MSCs passed through the membrane, whereas 82.7% of the MNCs traversed the smaller 5-μm pores. The p_{yield} for rat MSCs was 0.49 ± 0.07 mm Hg (n = 9, Figure 2b); the diameter of cells downstream of the filter was 15.6 ± 0.9 μm, corresponding to a cortical tension of 0.52 ± 0.03 dyne/cm for MSCs (P = NS versus MNCs). To confirm that we could detect differences in cell deformability if they existed, experiments were conducted after treating MSCs with cytochalasin B, which significantly decreased the cortical tension (0.16 ± 0.04 dyne/cm, n = 5, $P<0.05$ versus untreated MSCs; Figure 2c). After exposure to oxidative stress (H_2O_2), a nonsignificant increase in MSC stiffness was observed (Figure 2c).

Chronic Fate of Arterially Injected MSCs

Figure 3 depicts the entrapped cell density in rats studied acutely, 24 and 72 hours (n = 6 to 7 per group) following intraarterial MSC delivery. By 72 hours, the number of MSCs within the cremaster muscle decreased to 14% of that seen immediately postinjection ($P<0.05$). After arterial injection of fluorescent MSCs that were rendered nonviable after exposure to oxidative stress, the number of fluorescent cells (0.2 ± 0.1 cells per field) seen at 24 hours was significantly less than that seen after viable MSC injection (6.9 ± 1.5 cells per field, $P<0.01$; Figure 3), confirming that persistent dye does not transfer between dying MSCs and adjacent cells.

In vivo labeling of the microvessel basement membrane with rhodamine-labeled BSL I indicated that by 24 hours, the intact MSCs underwent significant conformational change, with spreading on the luminal side of the microvessels. Flow was restored in most microvessels containing MSCs (Figure 4b). At 72 hours, MSCs were seen in a perivascular location outside of, or embedded in, the microvascular basement membrane (Figures 4c and 5c). The persisting MSCs were integrated into the microvessel wall only at the precapillary level, indicating that MSC integration occurred at the level of initial entrapment.

The MSC nuclear double-stranded DNA was stained in 4 additional rats before arterial injection. At 24 hours following injection, a lesser proportion of cells showed preserved nuclear morphology (Figure 5a), whereas most cells exhibited cytoplasmic fragmentation and nuclear condensation (Figure 5b), indicative of cell death. At 72 hours, the limited number of cells that persisted in the cremaster muscle had preserved nuclear morphology, suggestive of cell viability up to that time point (Figure 5c).

Discussion

Our data indicate that the majority of systemically delivered MSCs arrest at the precapillary level, resulting in cessation of flow in the microvessel and flow reduction in the feeding arteriole. Studies in large animals[8,9] have shown that intracoronary delivery of MSCs leads to microinfarctions, whereas with IV infusion, most cells are trapped in the lungs.[10,11] We provide direct evidence that this is attributable to precapillary MSC entrapment. This is likely a mechanical phenomenon, because MSC entrapment invariably occurred in microvessels smaller in caliber compared to the cells. We did not observe arteriolar MSC adhesion, such as that described with cancer cells in similar intravital microscopy studies.[17] Unlike prior studies demonstrating increased lung clearance of MSCs with administration of SNP,[10] this was not the case in the cremaster microcirculation, probably related to the reduced caliber of the pathways selectively dilated by SNP in this preparation.[18]

Applying a method used to measure leukocyte deformability to evaluate this property in MSCs,[16] we confirmed that MSCs were as deformable as circulating MNCs (Figure 2c). Nonetheless, only a limited number of MSCs were able to traverse through 10-μm pores (Figure 2a), further supporting the concept that precapillary MSC entrapment in vivo is a mechanical phenomenon. Importantly, the rat cells used in this study were expanded to a similar degree as the human MSCs currently used in clinical trials. Intraarterial injection of human MSCs (Cambrex/Osiris, 20-μm mean diameter in our laboratory) led to similar microvascular plugging in the rat cremaster (data not shown). We posit that the large cell size is a direct consequence of the culture techniques, because freshly isolated human MSCs are smaller in size (≈10-μm diameter[19]). Different methods of MSC expansion may retain the original cell size in the marrow[20] and could result in improved intravascular rheology.

The tissue integration of entrapped MSCs observed in this study was a slower process compared to that reported for leukocyte transmigration,[21] extending over 24 to 72 hours (Figure 6). The entrapped MSCs spread on the luminal surface by 24 hours (Figures 4a, 4b, and 5a), in agreement with electron microscopy data reporting initial MSC integration within the endothelial layer.[11,22] The ischemia caused by microvascular plugging is likely responsible for the cell death observed at this time point, as indicated by the predominant cell/nuclear fragmentation at 24 hours (Figure 4b). By 72 hours, the surviving MSCs integrate into a perivascular/intramural location, reminiscent of pericytes (Figures 4c and 5c). This is in agreement with the recent reports of MSC-like cells in perivascular locations in various tissues,[23,24] which may function as a reservoir of tissue-specific regenerative cells. We did not investigate the fate of the entrapped MSCs beyond 3 days; however, we have previously shown that a very limited number of systemically delivered human MSCs survive long term and adopt a myocyte phenotype in the mouse myocardium.[25] Although we did not specifically explore the fate MSCs in the injured tissue, cell size relative to microvessel size will also likely play a determining role in the initial biodistribution and cell fate.

In summary, when delivered systemically most culture-expanded MSCs became mechanically entrapped at the precapillary level. This leads to significant flow reduction, with predominant MSC death and a small number of cells integrating in a perivascular

niche. Given that microvascular architecture is universally conserved across most organ beds, our findings in the cremaster model likely translate to other microvascular beds, as well. To enhance therapeutic success, while avoiding microembolization, future efforts should explore conditions that will preserve the putative ability of native MSCs to circulate and actively engraft.

Supplementary Material

Refer to Web version on PubMed Central for supplementary material.

Acknowledgments

We thank Jason Shields (Olympus) for help with microscopy and Joan Gretton for administrative assistance.

Sources of Funding

This work was supported, in part, by the University of Pittsburgh Medical Center, a Scientist Development Grant from the American Heart Association (to C.T.), and the National Institutes of Health (to F.V.).

References

1. Caplan AI, Dennis JE. Mesenchymal stem cells as trophic mediators. J Cell Biochem. 2006; 98:1076–1084. [PubMed: 16619257]
2. Gnecchi M, He H, Noiseux N, Liang OD, Zhang L, Morello F, Mu H, Melo LG, Pratt RE, Ingwall JS, Dzau VJ. Evidence supporting paracrine hypothesis for Akt-modified mesenchymal stem cell-mediated cardiac protection and functional improvement. FASEB J. 2006; 20:661–669. [PubMed: 16581974]
3. Pittenger MF, Mackay AM, Beck SC, Jaiswal RK, Douglas R, Mosca JD, Moorman MA, Simonetti DW, Craig S, Marshak DR. Multilineage potential of adult human mesenchymal stem cells. Science. 1999; 284:143–147. [PubMed: 10102814]
4. Jones E, McGonagle D. Human bone marrow mesenchymal stem cells in vivo. Rheumatology (Oxford). 2008; 47:126–131. [PubMed: 17986482]
5. Le Blanc K, Frassoni F, Ball L, Locatelli F, Roelofs H, Lewis I, Lanino E, Sundberg B, Bernardo ME, Remberger M, Dini G, Egeler RM, Bacigalupo A, Fibbe W, Ringdén O. Mesenchymal stem cells for treatment of steroid-resistant, severe, acute graft-versus-host disease: a phase II study. Lancet. 2008; 371:1579–1586. [PubMed: 18468541]
6. Chen SL, Fang WW, Ye F, Liu YH, Qian J, Shan SJ, Zhang JJ, Chunhua RZ, Liao LM, Lin S, Sun JP. Effect on left ventricular function of intracoronary transplantation of autologous bone marrow mesenchymal stem cell in patients with acute myocardial infarction. Am J Cardiol. 2004; 94:92–95. [PubMed: 15219514]
7. Katritsis DG, Sotiropoulou PA, Karvouni E, Karabinos I, Korovesis S, Perez SA, Voridis EM, Papamichail M. Transcoronary transplantation of autologous mesenchymal stem cells and endothelial progenitors into infarcted human myocardium. Catheter Cardiovasc Interv. 2005; 65:321–329. [PubMed: 15954106]
8. Vulliet PR, Greeley M, Halloran SM, MacDonald KA, Kittleson MD. Intra-coronary arterial injection of mesenchymal stromal cells and micro-infarction in dogs. Lancet. 2004; 363:783–784. [PubMed: 15016490]
9. Freyman T, Polin G, Osman H, Crary J, Lu M, Cheng L, Palasis M, Wilensky RL. A quantitative, randomized study evaluating three methods of mesenchymal stem cell delivery following myocardial infarction. Eur Heart J. 2006; 27:1114–1122. [PubMed: 16510464]
10. Gao J, Dennis JE, Muzic RF, Lundberg M, Caplan AI. The dynamic in vivo distribution of bone marrow-derived mesenchymal stem cells after infusion. Cells Tissues Organs. 2001; 169:12–20. [PubMed: 11340257]
11. Barbash IM, Chouraqui P, Baron J, Feinberg MS, Etzion S, Tessone A, Miller L, Guetta E, Zipori D, Kedes LH, Kloner RA, Leor J. Systemic delivery of bone marrow-derived mesenchymal stem

cells to the infarcted myocardium: feasibility, cell migration, and body distribution. Circulation. 2003; 108:863–868. [PubMed: 12900340]

12. Rüster B, Göttig S, Ludwig RJ, Bistrian R, Müller S, Seifried E, Gille J, Henschler R. Mesenchymal stem cells display coordinated rolling and adhesion behavior on endothelial cells. Blood. 2006; 108:3938–3944. [PubMed: 16896152]
13. Segers VF, Van Riet I, Andries LJ, Lemmens K, Demolder MJ, De Becker AJ, Kockx MM, De Keulenaer GW. Mesenchymal stem cell adhesion to cardiac microvascular endothelium: activators and mechanisms. Am J Physiol Heart Circ Physiol. 2006; 290:H1370–H1377. [PubMed: 16243916]
14. Steingen C, Brenig F, Baumgartner L, Schmidt J, Schmidt A, Bloch W. Characterization of key mechanisms in transmigration and invasion of mesenchymal stem cells. J Mol Cell Cardiol. 2008; 44:1072–1084. [PubMed: 18462748]
15. Baez S. An open cremaster muscle preparation for the study of blood vessels by in vivo microscopy. Microvasc Res. 1973; 5:384–394. [PubMed: 4709735]
16. Eppihimer MJ, Lipowsky HH. The mean filtration pressure of leukocyte suspensions and its relation to the passage of leukocytes through nuclepore filters and capillary networks. Microcirculation. 1994; 4:237–250. [PubMed: 8790593]
17. Glinskii OV, Huxley VH, Glinsky GV, Pienta KJ, Raz A, Glinsky VV. Mechanical entrapment is insufficient and intercellular adhesion is essential for metastatic cell arrest in distant organs. Neoplasia. 2005; 7:522–527. [PubMed: 15967104]
18. Mustafa SS, Rivers RJ, Frame MD. Microcirculatory basis for non-uniform flow delivery with intravenous nitroprusside. Anesthesiology. 1999; 91:723–731. [PubMed: 10485784]
19. Gronthos S, Zannettino AC, Hay SJ, Shi S, Graves SE, Kortesidis A, Simmons PJ. Molecular and cellular characterization of highly purified stromal stem cells derived from human bone marrow. J Cell Sci. 2003; 116:1827–1835. [PubMed: 12665563]
20. Baksh D, Zandstra PW, Davies JE. A non-contact suspension culture approach to the culture of osteogenic cells derived from a CD49elow subpopulation of human bone marrow-derived cells. Biotechnol Bioeng. 2007; 98:1195–1208. [PubMed: 17614333]
21. Habazettl H, Lindert J, Baeter S, Neumann K, Kuppe H, Kuebler WM, Pries AR, Koster A. Effects of unfractionated heparin, low molecular weight heparin and r-hirudin on leukocyte adhesion in ischemia/reperfusion. Blood Coagul Fibrinolysis. 2004; 15:375–381. [PubMed: 15205585]
22. Schmidt A, Ladage D, Steingen C, Brixius K, Schinkothe T, Klinz FJ, Schwinger RH, Mehlhorn U, Bloch W. Mesenchymal stem cells transmigrate over the endothelial barrier. Eur J Cell Biol. 2006; 85:1179–1188. [PubMed: 16824647]
23. Dellavalle A, Sampaolesi M, Tonlorenzi R, Tagliafico E, Sacchetti B, Perani L, Innocenzi A, Galvez BG, Messina G, Morosetti R, Li S, Belicchi M, Peretti G, Chamberlain JS, Wright WE, Torrente Y, Ferrari S, Bianco P, Cossu G. Pericytes of human skeletal muscle are myogenic precursors distinct from satellite cells. Nat Cell Biol. 2007; 9:255–267. [PubMed: 17293855]
24. Crisan M, Deasy B, Gavina M, Zheng B, Huard J, Lazzari L, Péault B. Purification and long-term culture of multipotent progenitor cells affiliated with the walls of human blood vessels: myoendothelial cells and pericytes. Methods Cell Biol. 2008; 86:295–309. [PubMed: 18442653]
25. Toma C, Pittenger MF, Cahill KS, Byrne BJ, Kessler PD. Human mesenchymal stem cells differentiate to a cardiomyocyte phenotype in the adult murine heart. Circulation. 2002; 105:93–98. [PubMed: 11772882]

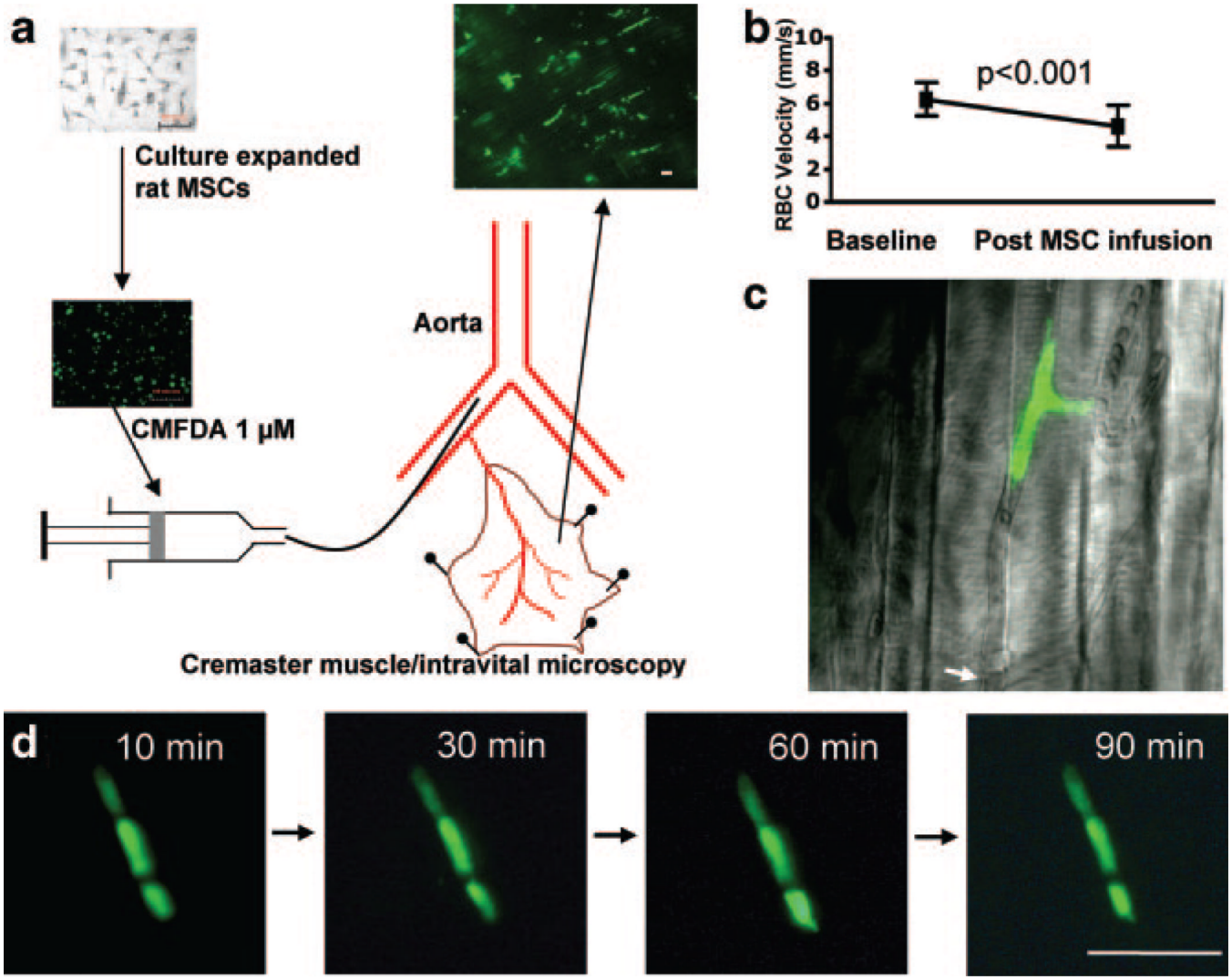

Figure 1.

Rheological effects of intraarterially delivered MSCs. a, MSCs fluorescently labeled with CMFDA were injected above the origin of the cremaster artery, leading to diffuse precapillary cell entrapment. b, Microvascular plugging significantly decreased the RBC velocity in the feeding arteriole. c, High magnification of MSCs arrested in a microvessel with interruption of flow (arrow indicating the flow divergence point; see supplemental Video 1). d, Three entrapped MSCs observed for up to 90 minutes: no morphological changes suggestive of extravascular migration. Scale bar = 100 μm.

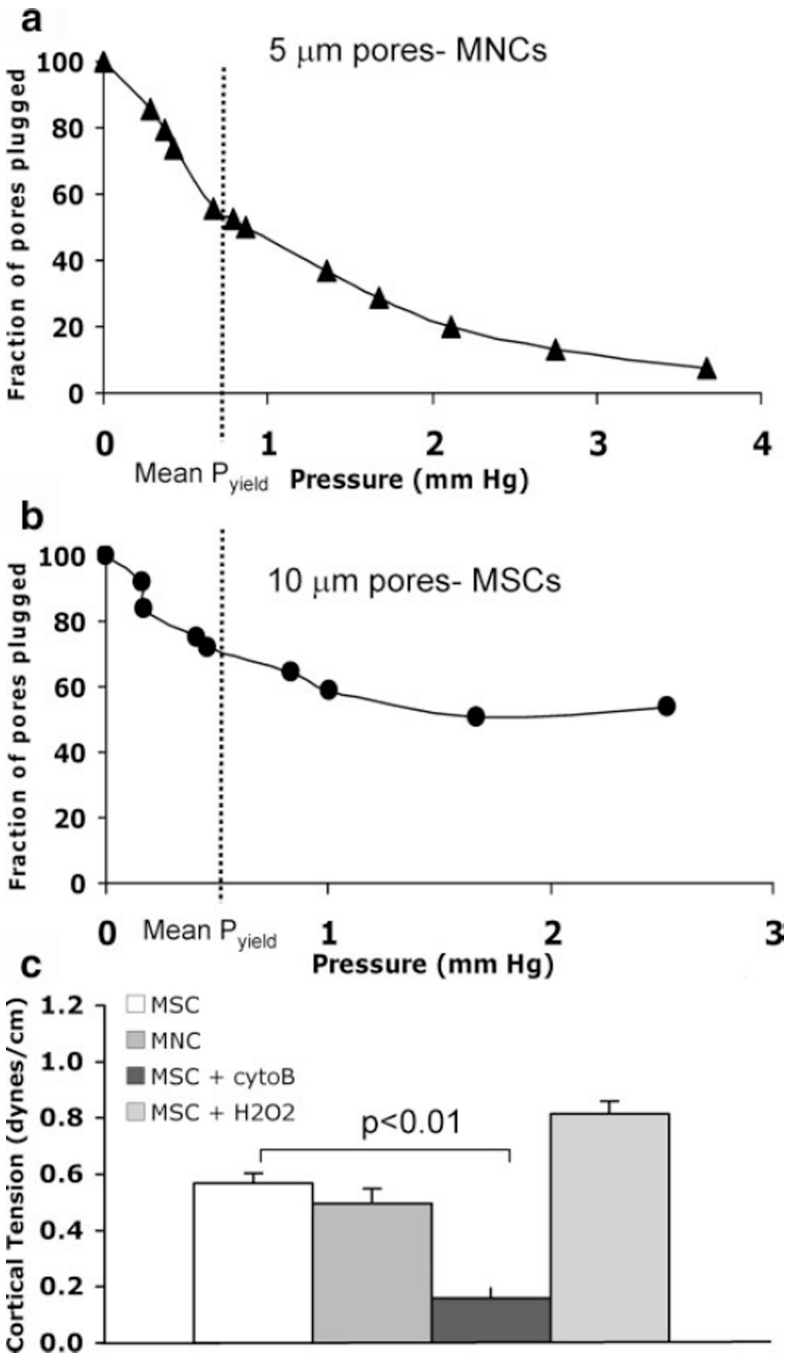

Figure 2.

Physical properties of MSCs. a and b, Ramp–filtration curves from experiments to measure deformability of MNCs and MSCs, respectively. c, Cortical tensions (stiffness) of MSCs and circulating MNCs were comparable; after disrupting the MSC cytoskeleton with cytochalasin B (cytoB), MSC cortical tension decreased. After oxidative stress (H_2O_2), cell stiffness nonsignificantly increased.

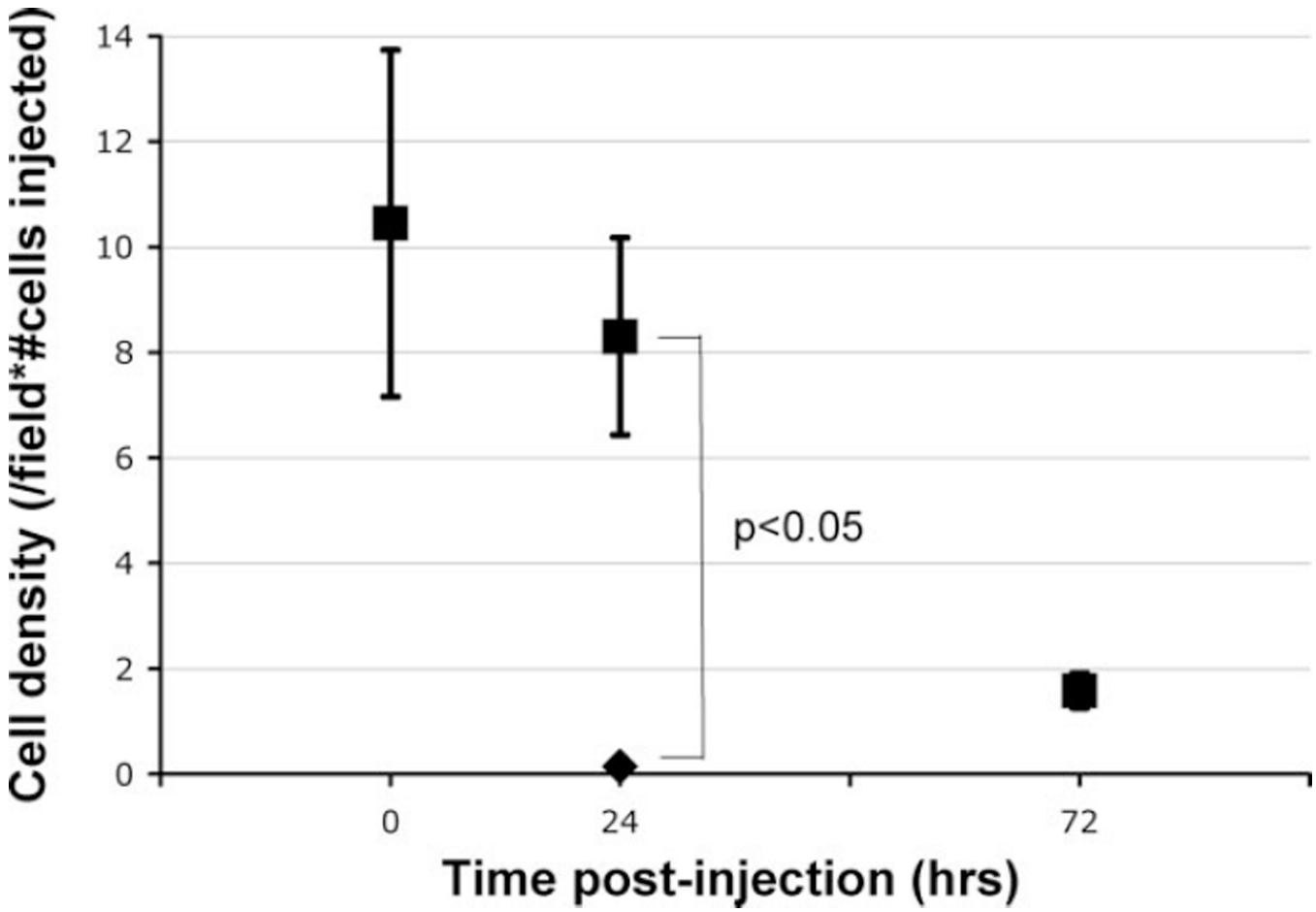

Figure 3.

Time course of MSC persistence in cremaster microcirculation. The density of fluorescent cells (numbers of cells/field normalized to the number of injected cells in millions) decreased significantly over time (■); when MSCs underwent oxidative stress (H_2O_2) to induce apoptosis, virtually no cells were identified at 24 hours (◆) (n = 3, $P<0.05$), indicating that the remaining fluorescent cells were MSCs and not an artifact from dye transfer.

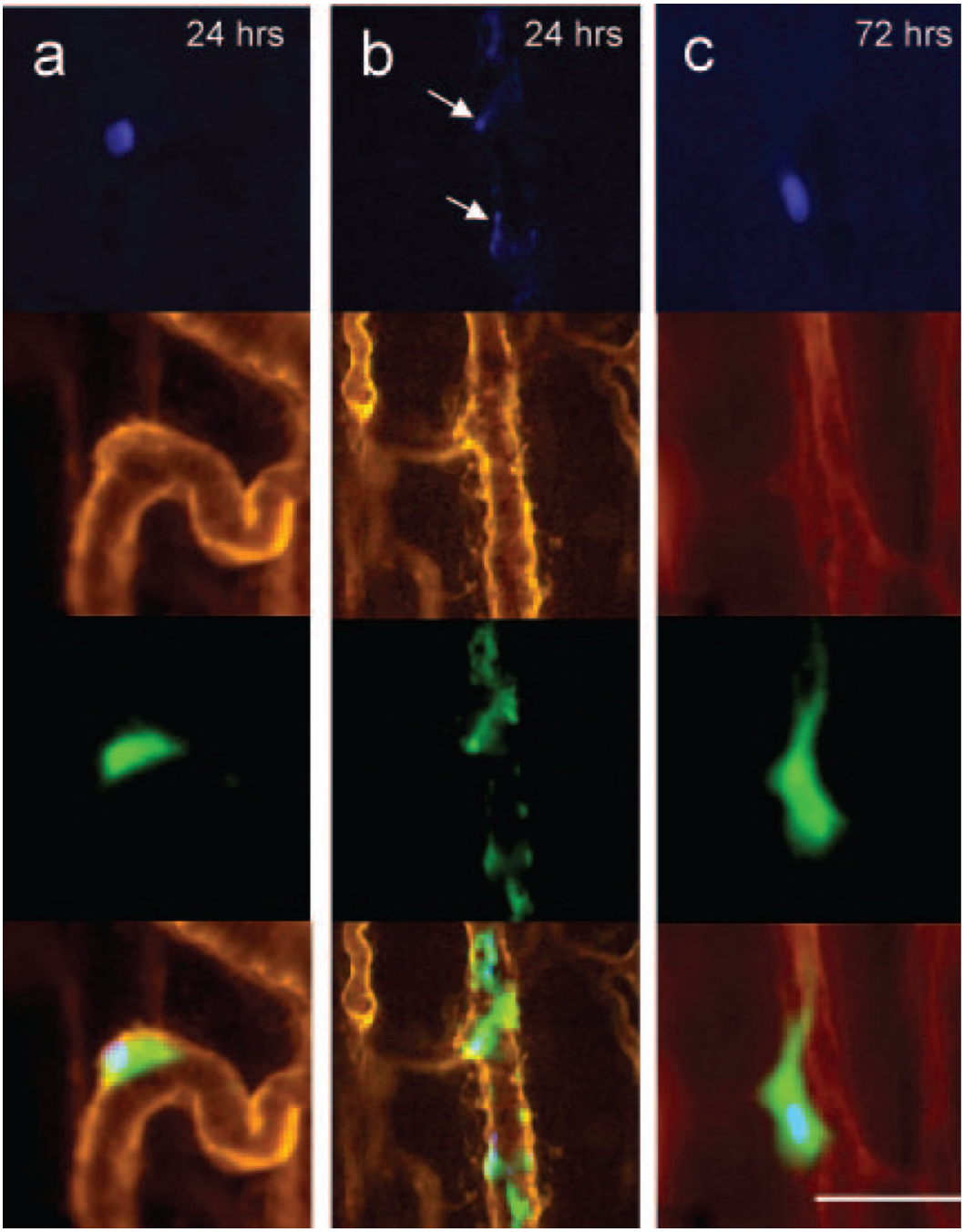

Figure 4.

Initial fate of entrapped cells. Multicolor in vivo fluorescence imaging of MSCs in cremaster muscle. The CMFDA-labeled MSCs are green fluorescent (third row), whereas the microvascular basement membrane was stained red with rhodamine-labeled BSL I (second row). The MSCs were double-labeled with DAPI for nuclear staining (blue, top row). The bottom rows represent fused images. a, At 24 hours, the MSCs were spread out on the luminal side of the microvessels with preserved cytoplasmic and nuclear morphology. b, Heavily fragmented cells at 24 hours, with nuclear condensation (arrows) suggestive of apoptosis. c, At 72 hours, most persisting cells were morphologically intact, with preserved nuclear morphology. Scale bar = 50 μm.

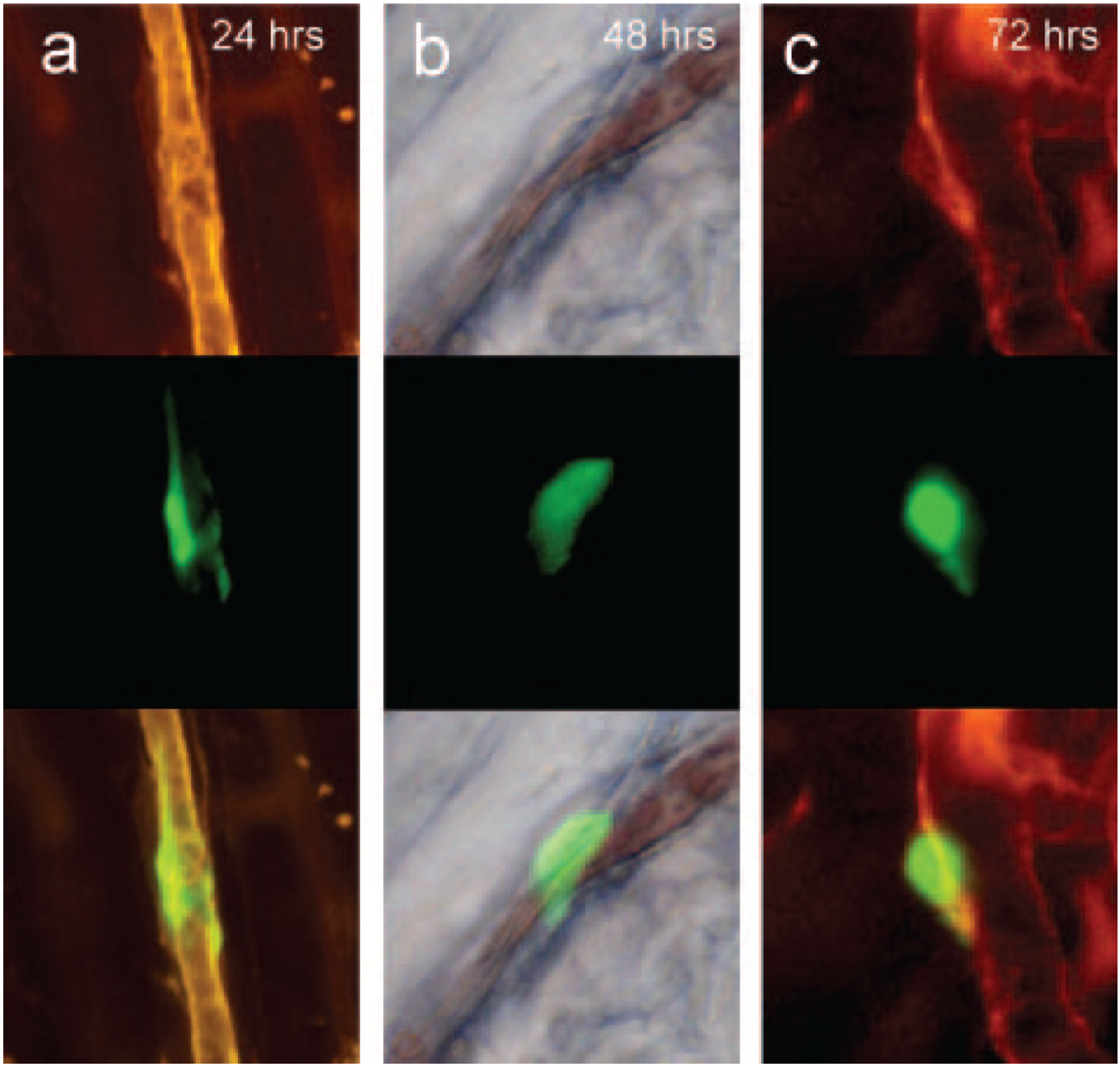

Figure 5.
MSC localization relative to the vessel wall. Multicolor in vivo fluorescence imaging of MSCs and basement membrane in the cremaster muscle, as in Figure 4. At 24 to 48 hours, the cells were spread out on the luminal side (a and b), with restoration of flow (depicted by the column of blood in the middle of column b, representing DIC imaging at 48 hours). At 72 hours, some of the cells appear perivascular, with presence of a basement membrane between the MSC and the microvessel (c). Scale bar = 50 μm.

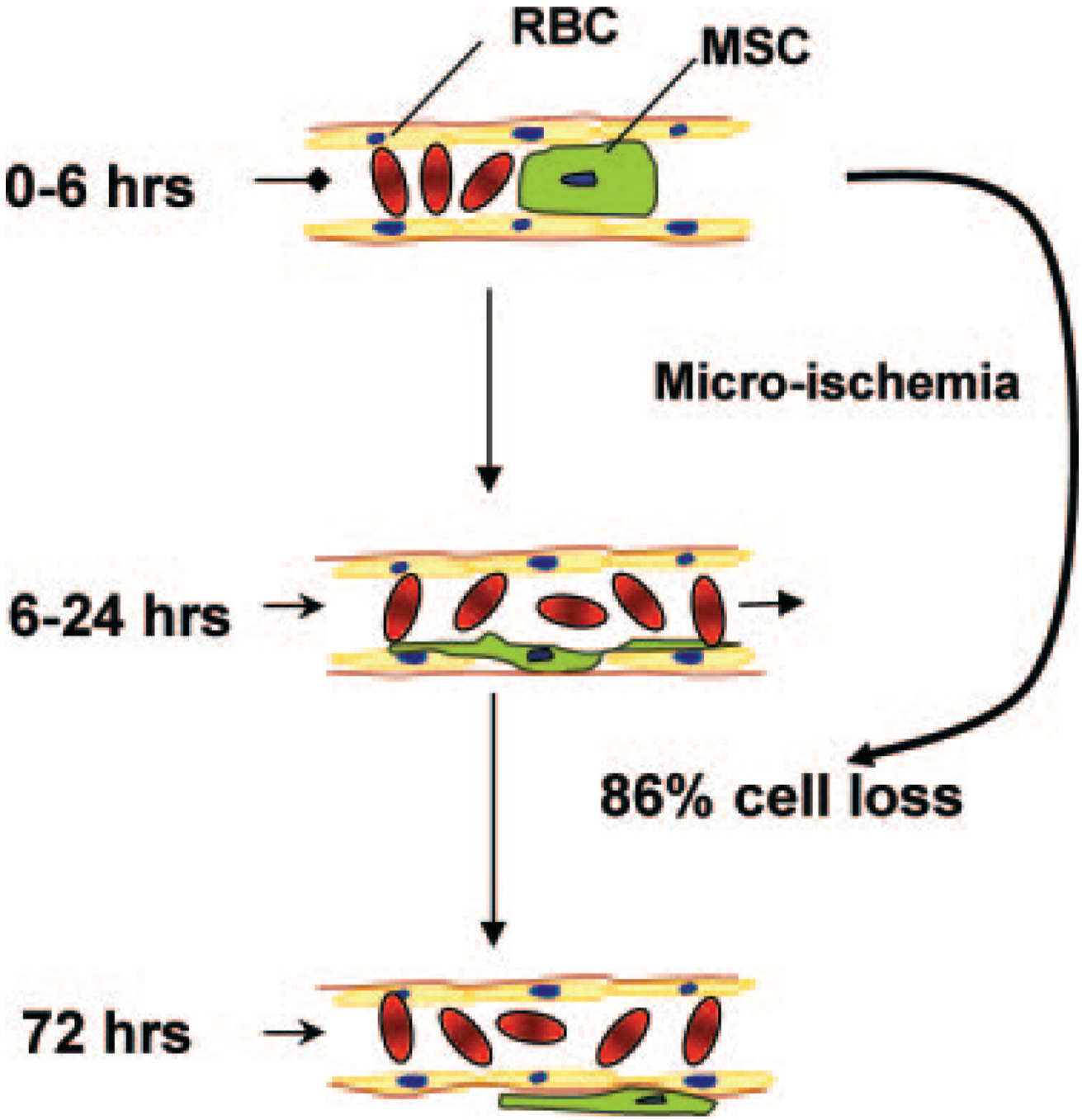

Figure 6.
Hypothesis for the intravascular fate of culture-expanded MSCs. After intraarterial MSC injection, microvascular plugging with obstruction of flow occurs at the precapillary level. The resulting ischemia leads to loss of most of the injected cells (86%). The few surviving cells initially spread out on the luminal side of the vessel and then localize in a perivascular niche.